Pure Appl. Geophys.

Pure and Applied Geophysics

Shallow Lake GPR Applications using an Autonomous Surface Vehicle

D. Dudziak,[1] T. Kufner,[1] and A. Crix [1]

Abstract—Underwater mapping is traditionally performed using sonar systems for bathymetric surveys and sub-bottom profilers for imaging subsurface stratigraphy. An alternative method for underwater mapping involves using ground penetrating radar (GPR). Limited research has been conducted with this approach because of the attenuation of electromagnetic waves in water, reducing the capability. However, if proven effective in certain conditions, this method would provide higher resolution multi-parameter imaging and allow for data collection in less accessible areas. This study aims to investigate the feasibility and effectiveness of integrating GPR with an autonomous surface vehicle (ASV) to acquire bathymetric and stratigraphic data in shallow lake environments. The method involved retrofitting an ASV with GPR equipment and conducting a survey in the Inner Harbour of Kingston, Ontario. The data collected from three separate tests was processed using MALÅ Vision and the path was recorded using the GPS system on an iPhone attached to the ASV. The GPR signal penetrated to depth of 1.75m and resolved the bathymetry, stratigraphic layering, and indications of buried objects. The results demonstrate that GPR is a promising alternative for collecting data in shallow water environments and the benefits and limitations of this approach are discussed.

Keywords: Ground Penetrating Radar, Autonomous Surface Vehicle, Shallow-Lake, Bathymetry

1. Introduction

The primary objective of this project is to evaluate the feasibility of using an autonomous surface vehicle (ASV) to collect ground penetrating radar (GPR) data in shallow lake environments. While GPR has previously been applied to lakes for bathymetric and stratigraphic surveys, data collection has typically relied on manually operated vessels, such as the study conducted by Sambuelli and Bava (2012) on a morainic lake in Italy (Sambuelli, 2012). This work seeks to extend prior efforts by investigating an ASV-based approach. Secondary objectives include mapping sediment stratigraphy and assessing whether subsurface features—such as pipelines, cables, or shipwrecks—can be resolved within/above the sediment bed using waterborne GPR. This study focuses on evaluating feasibility rather than optimizing antenna configuration or survey parameters.

The survey was conducted in the Inner Harbour of Kingston, Ontario (Figure 1). This location is a shallow-water environment, with pre-existing bathymetric mapping indicating a maximum depth of approximately 0.9 m. The calm conditions, shallow water, and accessible shoreline made this site a favourable location for testing GPR signal penetration in a lake environment.

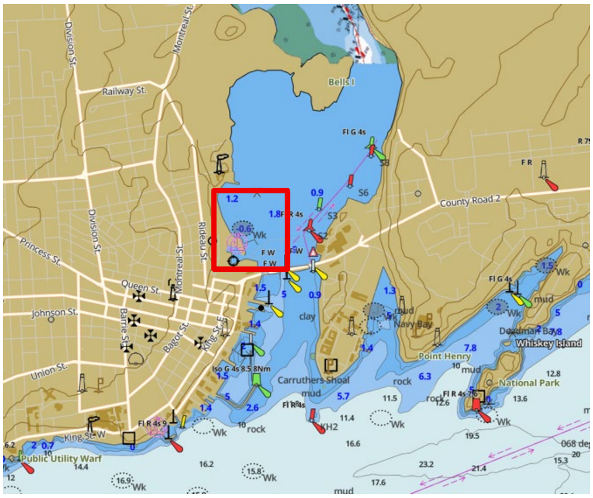

Figure 1
Location of the survey area in the Inner Harbour of Kingston, Ontario, showing pre-existing bathymetry. Red box indicates survey area. Modified from https://fishing-app.gpsnauticalcharts.com/i-boating-fishing-web-app/fishing-marine-charts-navigation.html?title=Kingston+Harbour+and+Approaches%5Cet+les+approches+boating+app#13/44.2330/-76.4851

In addition, the Inner Harbour contains documented anthropogenic features, including multiple shipwrecks submerged beneath the water surface. This made the site well suited for evaluating whether waterborne GPR is effective at resolving discrete objects located within or beneath the sediment bed. The availability of pre-existing bathymetric data was also beneficial, as it provided a useful reference against which the GPR-derived bathymetry could be compared and validated. The combination of these factors made the Inner Harbour an appropriate test site for this study.

The planned survey focused on performing horizontal transects parallel to the shoreline, with a localized survey grid positioned over one of the known shipwrecks (Figure 2). This approach was selected to evaluate the ability of the ASV-mounted GPR system to capture both continuous bathymetric variation along the shoreline and localized responses associated with

[1] Department of Geological Engineering, Faculty of Applied Science, Queen's University, Kingston, ON K7L 3N6, Canada. E-mail addresses: d.crix@queensu.ca, daniel.dudziak@queensu.ca, 20tjk2@queensu.ca

discrete submerged features.

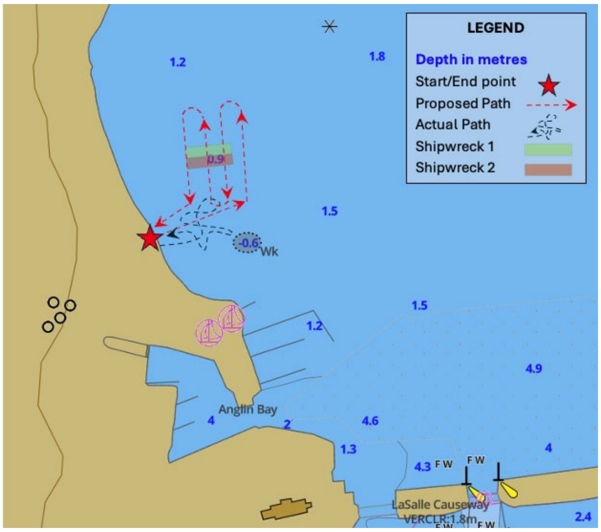

Figure 2
Proposed and actual ASV–GPR survey paths over a known shipwreck in the Inner Harbour of Kingston, Ontario. Modified from https://fishing-app.gpsnauticalcharts.com/i-boating-fishing-web-app/fishing-marine-charts-navigation.html?title=Kingston+Harbour+and+Approaches%5Cet+les+approches+boating+app#13/44.2330/-76.4851

2. *Methods*

The GPR System available to us was the MALÅ ProEx control unit equipped with a 250 MHz shielded antenna (Geo, 2022). The antenna's overall dimensions are 0.16m, and its mass is 7.85kg. Both the weight and surface area of the antenna were too large to integrate directly onto the ASV. Given this constraint, a secondary floatation platform was required to hold the GPR, while the ASV was used solely for its steering/propulsion. The secondary platform was towed behind the ASV during surveys.

The antenna's location resulted in design constraints as well. The general rule is that GPR antennas should be kept within at least 1/10 of the center frequency wavelength from the surface it is imaging, to reduce air reflection (Sensoft, n.d.). The antenna height was placed within 12cm of the surface of the water, with a more precise measurement not being obtained, however, 3-5cm from the surface would have been ideal (Sensoft, n.d.). Maintaining minimal separation between the antenna and the bottom of the flotation device became a fundamental design restraint. The separation distance margin became even smaller after accounting for the additional distance introduced by the air trapped in the bottom of the flotation device itself. A significant air gap would heavily affect our survey ability as it would result in signal broadening, reducing both our penetration depth and reduction in resolution.

This requirement is even further complicated by the large dielectric permittivity contrast between air (≈1) and water (≈80). Small separations or uneven contact could potentially lead to substantial reflection losses at the interface. Additionally, the setup required the surface below the antenna to remain relatively dry as any accumulation of water would also lead to signal degradation. These combined constraints motivated the use and Outbound 2-Person Inflatable boat as our flotation platform for the GPR (Outbound, 2025).

The inflatable boat proved to be very effective for this application. The boat was designed to inflate in three different sections independently, one being the bottom of the boat. This was helpful, as it allowed us to adjust the air gap between the antenna and the surface of the water. Too much air in the bottom section increased the separation distance, while too little air caused the antenna to sit below the waterline, resulting in reflections from the surrounding water. The GPR also fit almost perfectly inside the inflatable boat, requiring only pool noodles at the front and back to ensure a tight fit and prevent movement of the GPR during surveys (Figure 3).

Figure 3
ASV–GPR survey configuration during field testing, showing the GPR system mounted in the inflatable boat and towed behind the autonomous surface vehicle.

Reducing horizontal sway of the inflatable boat behind the ASV was also an important design consideration. Our survey plan consisted primarily of horizontal transects parallel to the shoreline, with less frequent vertical transects oriented perpendicular to it. This survey geometry was intended to provide dense coverage along the shoreline for bathymetric mapping and stratigraphic sectioning, while the perpendicular transects were included to improve detection of linear features, such as pipelines, oriented perpendicular to the coastline.

If the unpredictable lateral sway of the inflatable boat became too large, the effectiveness of this survey plan could be significantly reduced. While the ASV itself might follow the intended survey path accurately, the GPR system could deviate from that path, resulting in gaps or blind spots in the collected data and reducing overall survey coverage.

To address this concern, a V-shaped rope system (bridle) was added to the towing configuration. Ropes were tied from each handle of the inflatable boat to a central connection point on the towing line in front of the boat (Figure 3). This configuration was intended to reduce yawing caused by wind and wave effects while avoiding an overly rigid connection that could interfere with ASV steering.

In practice, this setup proved largely ineffective at reducing lateral sway. The handles used as attachment points were located too far toward the stern of the inflatable boat, resulting in minimal horizontal control and limited reduction in swaying caused by wind.

There was also concern regarding the magnitude of electromagnetic noise that could be produced by the ASV motors and its impact on the GPR data. To assess this, testing was conducted on land with the ASV motors running while the GPR system was positioned behind the boat. These tests showed no noticeable increase in background noise in the recorded GPR data. As a result, no strict minimum towing distance between the ASV and the inflatable boat was required to mitigate motor-related interference.

A phone was placed in the inflatable boat during each survey to collect GPS position data. By documenting the start time of each survey attempt, the GPR data could be correctly mapped to its true location along the shoreline (Figure 4). This positional information is essential for producing accurate bathymetric and stratigraphic maps of the surveyed area. On the survey day, three separate survey attempts were conducted using the ASV–GPR setup.

MalaVision was used to process the GPR data, which is an online software offered by the company Guideline Geo. The web version provides enough processing tools for this study's needs. The processing steps taken are outlined below, with information about the processing techniques found in Ciampoli et al.'s paper 'Signal Processing of GPR Data for Road Surveys.'

i. Since the GPR samples in time using two-way travel time, once the raw data files were uploaded to the software the output was changed to show a depth profile rather than a travel time profile.
ii. Then, the time-zero sample was set to 37. It is important to do this vertical offset step, so the data accurately shows the depth of reflections.
iii. Next, the velocity of the GPR signal was adjusted to match the signal speed in water, which is 33m/µs.
iv. Finally, various filters were applied (Table 1).

Table 1: Filters applied for GPR data processing through MalaVision, and their main effects on the data.

Filter Applied	Value	Purpose	Considerations
Aspect Ratio	1/2	Implemented to stretch the vertical axis and better see the measured layers.	Can lead to incorrect assumptions about sizes and spatial representation of features.
BG Removal	-	Remove horizontal banding which was present across the whole trace due to noise.	Sometimes, if perfectly horizontal layers are present, this filter could remove them by accident, but no such layers were expected for this survey.
Direct Current (DC) Offset	-	Removes the direct current noise introduced by the GPR.	The mean trace of a profile provides the average amplitude over that traces time-period, and with DC offset, that average is subtracted every trace, so every 0.1s, to remove any instrument bias.
Linear Gain	Slope of 1	Compensates for energy loss with depth, uses a linear amplitude multiplier	A slope of 1 is the smallest amount of gain possible in the MalaVision software, representing a very mild gain.
Automatic Gain Control (AGC)	-	Enhances weak reflectors by equalizing shallow and deep trace amplitudes	Could lead to interpretation of weak reflectors as significant features even if not as significant as initially stronger reflectors.
Contrast	550	Increases visual difference between bright and dark tones	Too much contrast can introduce unwanted artifacts.

3. *Results*

Three GPR surveys were executed with the ASV-GPR system, with survey paths for each test shown in Figure 4.

The GPR profiles from the three surveys along with features of note are shown in Figures 5-7. The depth imaged by the GPR was 1.75m in each of the surveys. Across these surveys, the bathymetry was successfully delineated, and the water depth was determined to be 0.0-0.8m across the survey area. Furthermore, in each of the surveys, additional features were imaged, indicated by clear parabolas in the GPR profile visible both before and after processing the data. Finally, a distinct sediment layer of unknown composition was noted at 1.25m in each of the surveys.

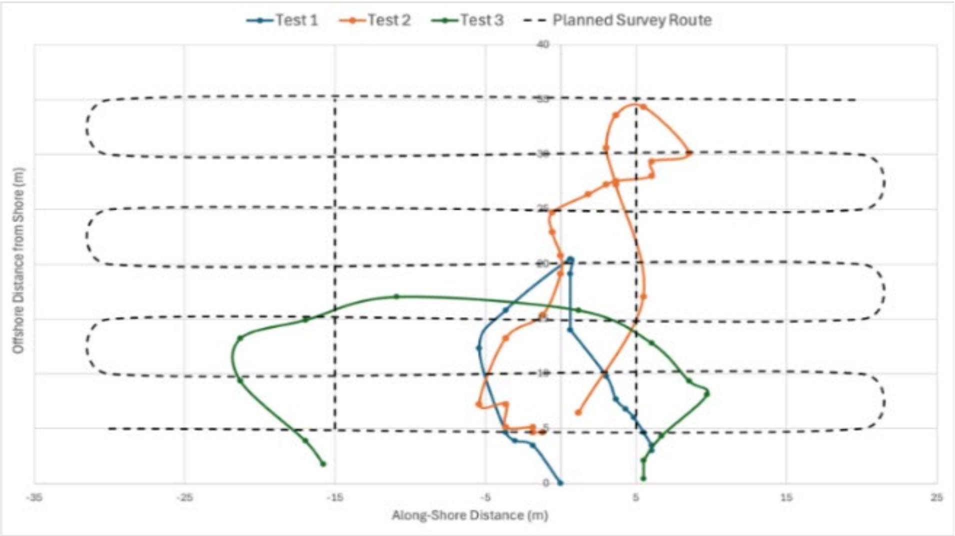

Figure 4
Paths taken by the ASV-GPR system at Inner Harbour, Kingston for 3 completed surveys. Different paths were attemped for each survey to mitigate weed exposure. Offshore distance (m) can be seen on the y-axis, while along-shore distance. (m) on the x-axis.

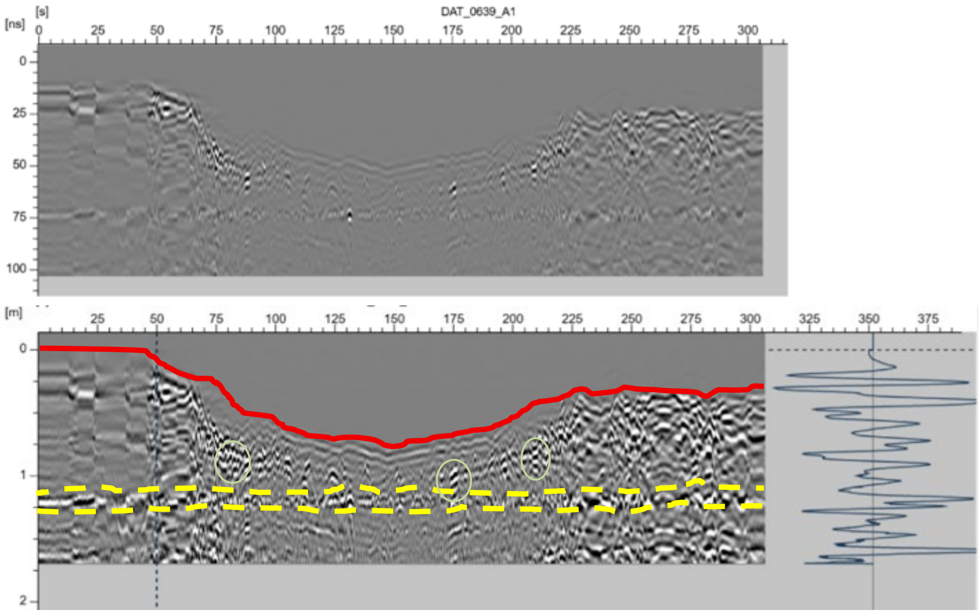

Figure 5
Unprocessed (top) and processed (bottom), GPR profiles for the first of three ASV-GPR surveys at Inner Harbour, Kingston. The unprocessed profile has DC offset, AGC, and Bg Removal applied, as is the default when importing into MalaVision. The y-axis is time (ns) for the unprocessed profile, and depth (m) for the processed profile, while the x-axis is time(s) for both. The red line indicates water surface, and dashed yellow line represents an unknown stratigraphic layer at a depth of ~1.25m. Other features of note are circled in green. GPR trace shown as a snapshot at 50s on the right side of the processed profile, representing a time slice before the ASV motors were tangled in weeds.

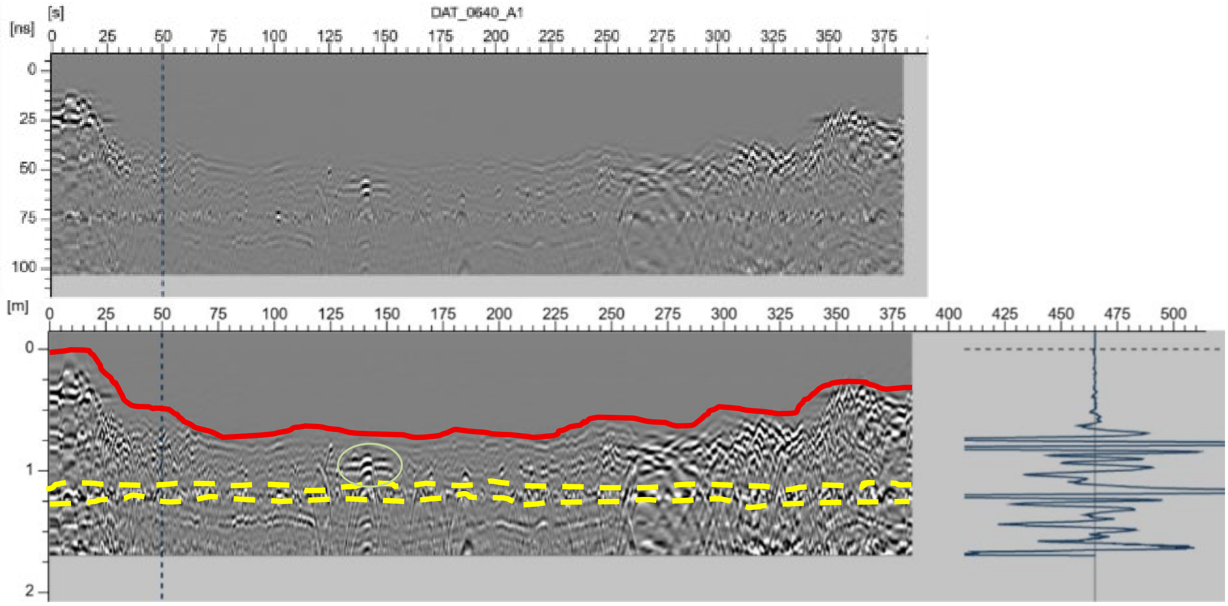

Figure 6

Unprocessed (top) and processed (bottom), GPR profiles for the second of three ASV-GPR surveys at Inner Harbour, Kingston. The unprocessed profile has DC offset, AGC, and Bg Removal applied, as is the default when importing into MalaVision. The y-axis is time (ns) for the unprocessed profile, and depth (m) for the processed profile, while the x-axis is time(s) for both. The red line indicates water surface, and dashed yellow line represents an unknown stratigraphic layer at a depth of ~1.25m. Other features of note are circled in green. GPR trace shown as a snapshot at 50s on the right side of the processed profile, representing a time slice before the ASV motors were tangled in weeds.

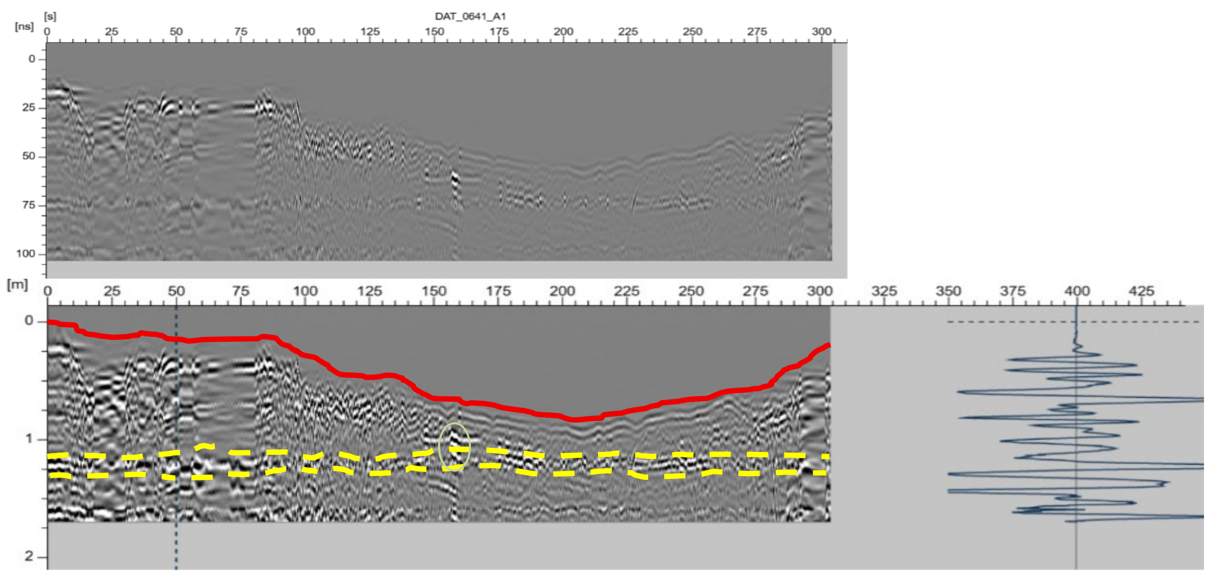

Figure 7

Unprocessed (top) and processed (bottom), GPR profiles for the third of three ASV-GPR surveys at Inner Harbour, Kingston. The unprocessed profile has DC offset, AGC, and Bg Removal applied, as is the default when importing into MalaVision. The y-axis is time (ns) for the unprocessed profile, and depth (m) for the processed profile, while the x-axis is time(s) for both. The red line indicates water surface, and dashed yellow line represents an unknown stratigraphic layer at a depth of ~1.25m. Other features of note are circled in green. GPR trace shown as a snapshot at 50s on the right side of the processed profile, representing a time slice before the ASV motors were tangled in weeds.

4. *Discussion*

Weeds in the study area posed a significant challenge during testing and prevented the ASV from following the desired path. Despite the challenges faced, the results are very promising. As shown in Figures 5-7, the GPR was able to successfully resolve the bathymetry and stratigraphy up to a depth of approximately 1.75m with good resolution. No reflections from the air-water boundary were evident in the results, indicating sufficient coupling between the GPR antenna and the water medium. This is expected since the distance between the GPR antenna and the water surface was minimized and within 1/10 of the center frequency wavelength of the antenna. Several key features were evident in the results including water depth, stratigraphic layering, and notable objects.

The water depth is clearly visible and marked by the red line in Figures 5-7 on the processed data for all three tests. The depth varied from 0m to 0.8m as the ASV traversed from the shore to slightly deeper water. GPS Nautical Charts were used to visualize and compare the rough bathymetry of the area to the data collected from the GPR survey. The water depth indicated was between 0.0-1.0m matching very well with the depth information from the GPR survey. The slight differences between the data are because the survey did not include the entire region of previously measured bathymetry. Attaching a depth sounder to the ASV would provide a more accurate comparison of the bathymetry but given the time constraints of this study a depth sounder could not be included. However, the results still indicate that the GPR can produce reasonable bathymetric data in shallow water environment.

The radargrams in each test also display a sharp contrast at approximately 1.25m below the surface, indicating a change in the subsurface sedimentary. The GPR is detecting a change in the dielectric constant which is consistent with the boundary between stratigraphic layers. The coefficient of reflection is shown in equation 2 and can be derived from the reflectance shown in equation 1, which describes the fraction of the incident waves power that is reflected at the interface (GeoSci Developers, 2025).

$$R = \frac{\overrightarrow{S_R} \cdot \hat{n}}{\overrightarrow{S_I} \cdot \hat{n}} = \left|\frac{E_{Ro}}{E_{Io}}\right|^2 \qquad (1)$$

$$R = \left|\frac{\sqrt{\widetilde{\varepsilon_2}} - \sqrt{\widetilde{\varepsilon_1}}}{\sqrt{\widetilde{\varepsilon_2}} + \sqrt{\widetilde{\varepsilon_1}}}\right|^2 \qquad (2)$$

The dielectric constants are complex due to the conductivity of the mediums at which the electromagnetic wave is propagating through. The sedimentary layer at 1.25m is likely to be a wet material, perhaps clay. Clay has a high dielectric constant, producing a strong dielectric contrast with the overlying sedimentary layer, likely sand. Deeper penetration would likely reveal additional layering and potentially the depth to the bedrock. Although the GPR signal is attenuated in water, increasing the listening time would allow it to resolve greater depths.

Perhaps the most promising indicator of the GPR’s capabilities in shallow water environments was that it was able to resolve objects below the sea floor. These objects are indicated on each radiogram with green circles. The exact shape and size of the objects are unknown, however due to the characteristic hyperbolic response shown on the radargrams, it is clear an object is present. A rough estimate of the position of each object can be obtained by correlating the GPR time data with the corresponding GPS position and time information. Figure 4 shows the paths of the GPR for each test and the solid dots indicate ten second time intervals, which can be used with the GPR time information to determine an approximate position. However, the approximate position would have a large uncertainty because the recorded start times for the GPR were accurate to the minute and the GPS data required significant interpolation. Accurate estimation of the position would require a planned GPR survey route and a more robust GPS system to precisely determine the GPR location. As a result, estimated positions of the objects were not included in this study. Although the positions of the objects are not accurately determined, this result from the study opens the door for more advanced research on subsurface mapping in shallow water environments using an ASV-GPR system.

This study demonstrates the feasibility of waterborne GPR for resolving bathymetric and stratigraphic features in shallow freshwater environments, despite practical limitations. Future work should quantify depth limitations through surveys in deeper water, and validate GPR interpretations using core samples and depth-sonar measurements to assess performance and effective detection ranges for a given antenna frequency.

References

Bianchini Ciampoli, L., Tosti, F., Economou, N., & Benedetto, F. (2019). Signal Processing of GPR Data for Road Surveys. Geosciences, 9(2), 96. https://doi.org/10.3390/geosciences9020096

Geo, G. (2022). *MALÅ ProEx control unit user manual*. Retrieved from https://guidelinegeo.com/wp-content/uploads/2022/06/MALA-ProEx-Control-Unit-User-Guide-June-2025.pdf

GeoSci Developers. (2025, December 17). *Basic Principles*. Retrieved from GPG: https://gpg.geosci.xyz/content/GPR/GPR_fundamental_principles.html

Google Earth. (2025, December 17). Retrieved from https://earth.google.com/web/

Outbound. (2025). *Outbound 2-Person Inflatable River Boat Set, Ages 6Y+*. Retrieved from Canadian Tire: https://www.canadiantire.ca/en/pdp/outbound-2-person-inflatable-river-boat-set-ages-6y-0798313p.html

Sambuelli, L. B. (2012). Case study: A GPR survey on a morainic lake in northern Italy for bathymetry, water volume and sediment characterization. *Journal of Applied Geophysics*, 48-56.

Sensoft. (n.d.). *Tips: How high can my GPR be off the ground? GPR survey: Scanning*. Retrieved from Sensoft: https://www.sensoft.ca/blog/tips-how-high-can-my-gpr-be-off-the-ground/